NEUROSCIENCE

Central amygdala NPBWR1 neurons facilitate social novelty seeking and new social interactions

Shingo Soya[1,2], Koji Toda[3], Katsuyasu Sakurai[1], Yoan Cherasse[1], Yuki C. Saito[1], Manabu Abe[4], Kenji Sakimura[4], Takeshi Sakurai[1,2]*

The formation of new social interactions is vital for social animals, but the underlying neural mechanisms remain poorly understood. We identified CeA^{Npbwr1} neurons, a population in central amygdala expressing neuropeptide B/W receptor-1 (NPBWR1), that play a critical role in these interactions. CeA^{Npbwr1} neurons were activated during encounters with unfamiliar, but not with familiar, mice. Manipulations of CeA^{Npbwr1} neurons showed that their excitation is essential for maintaining physical interactions with novel conspecifics. Activation of CeA^{Npbwr1} neurons alleviated social deficits induced by chronic social defeat stress, suggesting therapeutic potential. Conversely, overexpression of human *NPBWR1* in CeA^{Npbwr1} neurons reduced activity of these neurons and impaired social interactions with unfamiliar mice. This effect was absent in a polymorphic variant of the human NPBWR1 gene (404A>T). These findings highlight how CeA^{Npbwr1} neurons promote social novelty seeking and reveal a complex interplay between *NPBWR1* genetic variations and social behavior.

INTRODUCTION

The preference for social novelty is a common trait among mammalian species, implying an innate inclination to actively seek and establish new social interactions with unfamiliar individuals within their societies (*1*, *2*). Conversely, sociability deficits when interacting with new individuals are frequently observed in psychiatric conditions such as depression and autism (*3*, *4*). A similar phenotype is also evident in mouse models of these disorders (*5*, *6*), suggesting that the underlying mechanisms influencing social novelty preference may have common evolutionary origins.

While the neural correlates governing this function have not yet been identified, considering the function of the amygdala in assessing the emotional significance (*7*, *8*), salience (*9*), and valence (*10*–*12*) of the environmental stimuli, it is plausible that this structure also plays a role in processing the social novelty preference. We previously reported social and behavioral abnormalities in mice lacking neuropeptide B/W receptor 1 (NPBWR1), a receptor for neuropeptides B and W. These mice demonstrate impulsive interactions with unfamiliar mice, characterized by more intense approaches, prolonged contact, and extended chasing durations. *Npbwr1* is predominantly expressed in the lateral division of the central amygdala (CeA). These data suggest that NPBWR1 plays a critical role in regulating social behavior in the amygdala. This led us to investigate the role of *Npbwr1*-expressing neurons in social novelty preference. Previous research suggested that the amygdala likely plays a central role in this function, as evidenced by studies showing an impaired personal space response to new individuals in humans with bilateral amygdala lesions (*13*).

The CeA was previously recognized as a relay nucleus connecting the basolateral amygdala (BLA) to the brainstem. Recent studies have revealed intricate circuit mechanisms within the CeA, highlighting its involvement in defense responses and risk management and revealing more nuanced roles for this structure (*14*–*17*). In particular, we investigated the role of *Npbwr1*-expressing neurons within the CeA, which constitute a subpopulation of GABAergic neurons (CeA^{Npbwr1}) (*18*).

We previously found a connection between a single-nucleotide polymorphism (SNP, 404A>T) in the human *NPBWR1* gene, resulting in an amino acid change (Y135F), and altered emotional responses to human facial stimuli (*19*). This additional evidence further supports the hypothesis that CeA^{Npbwr1} neurons play a pivotal role in regulating behavior during social engagement, especially in the context of a preference for social novelty.

Here, we report that a distinct neural circuit consisting of CeA^{Npbwr1} neurons plays a critical role in regulating social novelty preference. These neurons were activated to maintain a close physical distance by inhibiting neurons in the brainstem that triggered escape behavior when mice made physical contact with stranger mice but not with familiar mice. By manipulating CeA^{Npbwr1} neurons in both directions, we observed a significant alteration in social novelty preference. Furthermore, we found that the activation of CeA^{Npbwr1} neurons reversed sociability deficits induced by chronic social defeat stress (CSDS) in mice. In addition, we provided evidence that an SNP (404A>T) in the human *NPBWR1* gene affects the activity of CeA^{Npbwr1} neurons, thereby influencing the modulation of social novelty preference in mice, raising the intriguing possibility that the SNP may also influence social and behavioral characteristics in humans.

RESULTS

CeA^{Npbwr1} neurons respond differently to unfamiliar and familiar mice

Npbwr1-deficient mice exhibit abnormal behavior when interacting with novel conspecifics, suggesting that NPBWR1 plays a role in regulating social behavior (*2*). This study also provides insight into the function of CeA^{Npbwr1} neurons in social novelty preference. To test this hypothesis, we examined how the activity of CeA^{Npbwr1} neurons is altered in response to social interactions. To specifically manipulate CeA^{Npbwr1} neurons and monitor their activity, we generated mice in which codon-improved Cre recombinase (*iCre*) was knocked-in into the *Npbwr1* allele (*Npbwr1*$^{+/Cre}$ mice) (Fig. 1A and fig. S1). Homozygous *Npbwr1*$^{Cre/Cre}$

[1]International Institute for Integrative Sleep Medicine (WPI-IIIS), University of Tsukuba, 1-1-1 Tennodai, Tsukuba, Ibaraki 3058575, Japan. [2]Institute of Medicine, University of Tsukuba, Tsukuba, Ibaraki 305-8575, Japan. [3]Department of Psychology, Keio University, 2-15-45, Mita, Minato-ku, Tokyo 108-8345, Japan. [4]Department of Animal Model Development, Brain Research Institute, Niigata University, Asahimachi, Chuoku, Niigata 951-8585 Japan.
*Corresponding author. Email: sakurai.takeshi.gf@u.tsukuba.ac.jp

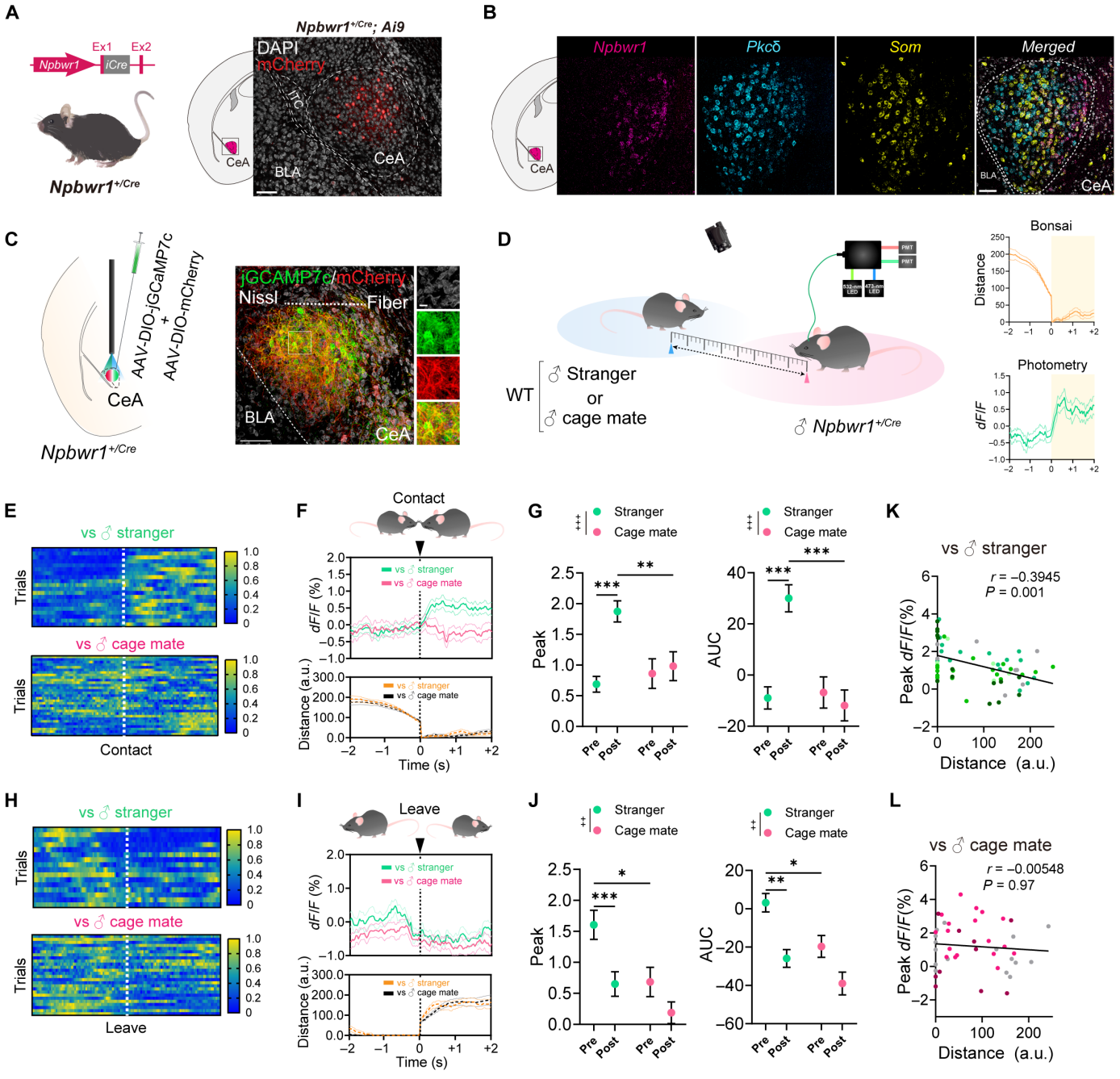

Fig. 1. Responsiveness of CeA^{Npbwr1} neurons to social novelty. (**A**) Distribution of Cre-expressing neurons in *Npbwr1*$^{+/Cre}$; *Ai9* mice visualized by tdTomato. Scale bar, 100 μm. (**B**) In situ hybridization in CeA. Panels show mRNA localizations for *Npbwr1* (magenta), *Pkc*δ (protein kinase delta, cyan), and *Som* (somatostatin, yellow). Scale bar, 50 μm. (**C**) Left: A drawing of AAV injection and optic fiber placement. Right: Representative image of jGCaMP7c and mCherry in CeA. Scale bars, 100 μm (left) and 200 μm (right). (**D**) Illustration of behavioral test of social interaction combined with fiber photometry and Bonsai. (**E**) Activity heat plot of jGCaMP7c signal from CeA^{Npbwr1} neurons in 2-s time windows before and after contact with a male stranger mouse (top) and a male cage mate (bottom). (**F**) Trial-averaged *dF/F* Ca^{2+} time course of CeA^{Npbwr1} neurons. Dotted lines show physical distance between mice. (**G**) Averaged peak *dF/F* Ca^{2+} and area under the curve (AUC) of (F). (**H**) Activity heat plot of jGCaMP7c signal from CeA^{Npbwr1} neurons 2 s before and after leaving with a male stranger mouse (top) and a male cage mate (bottom). (**I**) Trial-averaged *dF/F* Ca^{2+} time course of CeA^{Npbwr1} neurons. (**J**) Average peak *dF/F* Ca^{2+} and AUC. (**K**) Correlation between peak *dF/F* in CeA^{Npbwr1} neurons and social distance between test animals and male strangers. (**L**) Correlation between peak *dF/F* in CeA^{Npbwr1} neurons and social distance between test animals and male cage mate. Different colors correspond to each individual mouse. Spearman rank correlation. Data are from the *Npbwr1*$^{+/Cre}$ mice expressing jGCaMP7c in CeA^{Npbwr1} neurons. ($n = 5$, versus male stranger, 32 events for contact, 23 events for leaving; $n = 4$, versus male cage mate, 31 events for contact, 26 events for leaving). For the entire figure, bar graphs represent means ± SEM. $^{++}P < 0.01$, $^{+++}P < 0.001$, $^{*}P < 0.05$, $^{**}P < 0.01$, and $^{***}P < 0.001$. WT, wild type; PMT, photomultiplier tube; a.u., arbitrary units.

mice, which lacked the expression of *Npbwr1*, exhibited behavioral abnormalities characterized by increased physical interactions and decreased interindividual distance from novel conspecifics, consistent with our previous study (fig. S2) (*18*). Investigating the molecular identities of CeA^{Npbwr1} neurons by in situ hybridization showed that CeA^{Npbwr1} neurons were mostly GABAergic (*Vgat*; 94.6%), and many of them were colocalized with *Tac2* (*tachykinin*; 87.2%), *Nts* (*neurotensin*; 83.8%), *Pkc*δ (*protein kinase C delta*; 58.6%), and *Som* (*somatostatin*; 37.4%) (Fig. 1B and fig. S3), indicating that *Npbwr1* defines a distinct cellular population in the lateral part of the CeA (*20*).

To monitor the activity of CeA^{Npbwr1} neurons, we injected a Cre-dependent AAV (adeno-associated virus) vector carrying jGCaMP7c into the CeA of *Npbwr1*$^{+/Cre}$ mice (Fig. 1C) and observed fluorescence signals through an optical fiber implanted in the CeA. Social interactions were simultaneously analyzed using an automated program [Bonsai (*21*)] that tracked the physical distance between mice (Fig. 1D). The activity of CeA^{Npbwr1} neurons increased immediately after the social distance reached zero in male stranger mice (Fig. 1, E and F). In stark contrast, the activity of CeA^{Npbwr1} neurons did not change when the experimental mice faced familiar mice (male cage mates) (Fig. 1, E and F). Likewise, the responses of CeA^{Npbwr1} neurons decreased when the experimental mice were leaving the stranger mice but not when leaving the cage-mate mice (Fig. 1, H and I). The same tendency was observed when experimental mice faced female strangers (fig. S4, B to D). The activity of these neurons decreased when mice faced an object (toy mouse) (fig. S4, E to G). We found a significant negative correlation between the fluorescence level of CeA^{Npbwr1} neurons and physical distance to strangers but not to cage mates or toy mice (Fig. 1 and fig. S4). Furthermore, repeated exposure to male stranger mice gradually reduced the fluorescence response of CeA^{Npbwr1} neurons (fig. S5). These results suggested that the activity levels of CeA^{Npbwr1} neurons differed between novel and familiar individuals.

To elucidate the potential mechanisms underlying the differential activation of CeA^{Npbwr1} neurons in response to novel and familiar mice, we conducted retrograde tracing using a modified rabies virus (SAD-dG–GFP) (fig. S6). Our findings revealed that neurons synapsing directly onto CeA^{Npbwr1} neurons are distributed across various brain regions, as identified by this method. Notably, the primary input regions include the posterior BLA (pBLA), amygdalo-piriform transition area (AmPir), and ventral CA1 (vCA1). These results suggest that neurons in these regions modulate the activity of CeA^{Npbwr1} neurons in a manner dependent on whether the contacts are novel or familiar.

Manipulation of CeA^{Npbwr1} neurons alters preference for social novelty

To understand the physiological significance of CeA^{Npbwr1} neuron activation upon contact with novel conspecifics (Fig. 1, F and G), we conducted chemogenetic manipulations of CeA^{Npbwr1} neurons to investigate how alterations in their activity influenced social behavior. Initially, we examined the effect of excitatory chemogenetic manipulation of CeA^{Npbwr1} neurons on social behavior to understand the consequences of their activation, using a three-chamber social test (Fig. 2A). We injected a Cre-dependent AAV harboring hM3Dq-mCherry into the CeA of *Npbwr1*$^{+/Cre}$ mice (Fig. 2B). Intraperitoneal injection of

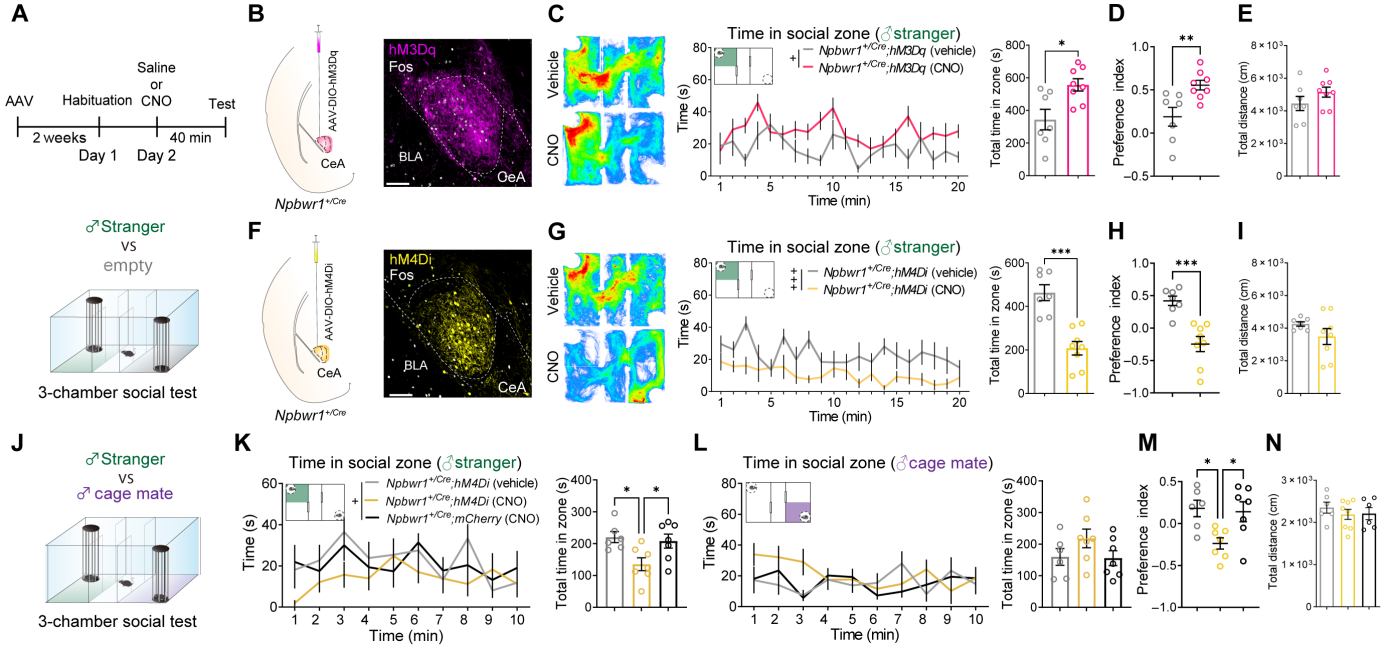

Fig. 2. Manipulation of CeA^{Npbwr1} neurons affects social novelty preference. (**A**) Experimental protocol. (**B**) Illustration showing AAV injection and immunohistochemical analysis showing hM3Dq-mCherry with c-Fos expression in the CeA after CNO administration. Scale bar, 100 μm. (**C**) Left: Heatmaps show the density of time spent in three-chamber. Right: Time spent in the social zone after CNO injection (hM3Dq) and total time spent in the social zone. Each dot is one mouse. (**D**) Preference index. Each dot is one mouse. (**E**) Total distance traveled of mice in (C). hM3Dq (vehicle): $n = 7$, hM3Dq (CNO): $n = 8$, mCherry (CNO): $n = 7$. (**F**) A schematic drawing of AAV injection and immunohistochemical analysis showing hM4Di-mCherry expression in the CeA. Scale bar, 100 μm. (**G**) Left: Heatmaps show the density of time spent in three-chamber. Right: Time spent in the social zone after CNO injection (hM4Di) and total time spent in the social zone. Each dot is one mouse. (**H**) Preference index. Vehicle: $n = 7$, CNO: $n = 8$. Each dot is one mouse. (**I**) Total distance traveled of mice in (G). (**J**) An illustration of a three-chamber social test with a male stranger and a cage mate. (**K**) Time spent in the social zone with a male stranger and total time. Each dot is one mouse. (**L**) Time in a social zone with a male stranger and total time. Each dot is one mouse. (**M**) Preference index. hM4Di (vehicle): $n = 7$, hM4Di (CNO: $n = 6$), mCherry (CNO: $n = 7$). (**N**) Total distance traveled of mice in (L). For the entire figure, bar graphs represent means ± SEM. $^{+}P < 0.05$, $^{+++}P < 0.001$, $^{*}P < 0.05$, $^{**}P < 0.01$, and $^{***}P < 0.001$.

clozapine *N*-oxide (CNO) into mice expressing hM3Dq-mCherry in CeA^{Npbwr1} neurons, which increased c-Fos expression in mCherry-expressing neurons (Fig. 2B), resulted in a significant increase in the time spent in the social zone in the three-chamber test using unfamiliar mice, without changing the total distance traveled (Fig. 2, C to E). This indicates that excitation of CeA^{Npbwr1} neurons leads to an increase in social interactions with novel conspecifics. This finding is consistent with the idea that NPBWR1, a Gi-coupled inhibitory receptor, inhibits physical contact in novel mice (*18*), and this effect is assumed to be mediated by the inhibition of CeA^{Npbwr1} neurons. Notably, we performed an elevated plus maze test combined with pharmacogenetic excitation of CeA^{Npbwr1} neurons using Cre-dependent AAV expressing hM3Dq (fig. S7). This experiment demonstrated that excitatory manipulation of these neurons did not affect anxiety in mice, suggesting that CeA^{Npbwr1} neurons are more likely to specifically alleviate social anxiety than induce a general anxiolytic effect.

Subsequently, we examined the effect of the chemogenetic inhibition of CeA^{Npbwr1} neurons, which might mimic the function of NPBWR1 (Fig. 2F). Inhibition of CeA^{Npbwr1} neurons by activating hM4Di resulted in a decrease in the time spent in the social zone compared to saline-injected control groups, without changing the total distance traveled (Fig. 2, G to I). These results suggest that activation of CeA^{Npbwr1} neurons upon encountering novel conspecifics facilitates social contact with opponents and that NPBWR1 serves as a negative regulator of this function.

Next, we evaluated social novelty preference using a three-chamber test with a cage mate and a stranger (Fig. 2J). Inhibition of CeA^{Npbwr1} neurons showed a significant decrease in the time spent in the zone with a stranger but an increased tendency with a cage mate (Fig. 2, K to M), without changing the total distance traveled (Fig. 2N).

Overall, these results indicate that CeA^{Npbwr1} neurons increase activity upon physical contact with strangers, and enhance social novelty preference. This mechanism may be essential for interacting with novel social individuals. Without this function, mice may not be able to make appropriate contact with strangers.

CeA^{Npbwr1} neurons act on a brain stem region to promote physical contact with strangers

Through virus-mediated tracing using a Cre-dependent AAV carrying an anterograde tracer, tdTomato-T2A-synaptophysin-GFP (*22*), we observed that CeA^{Npbwr1} neurons sent abundant axonal projections to the microcellular tegmentum (MiTg), lateral and medial parts of the parabrachial nucleus, lateral part of the substantia nigra pars lateralis (SNL), and nucleus solitarius (NTS) (Fig. 3, A and B). Notably, the axonal projections to the MiTg by CeA^{Npbwr1} neurons were particularly extensive, prompting us to investigate the functions of these projections (Fig. 3C). After expressing ChR2 in CeA^{Npbwr1} neurons by injecting Cre-dependent AAV into the CeA, we implanted optic fibers in the MiTg to perform excitatory manipulations (Fig. 3C). Excitation of CeA^{Npbwr1} fibers in the MiTg mice robustly increased

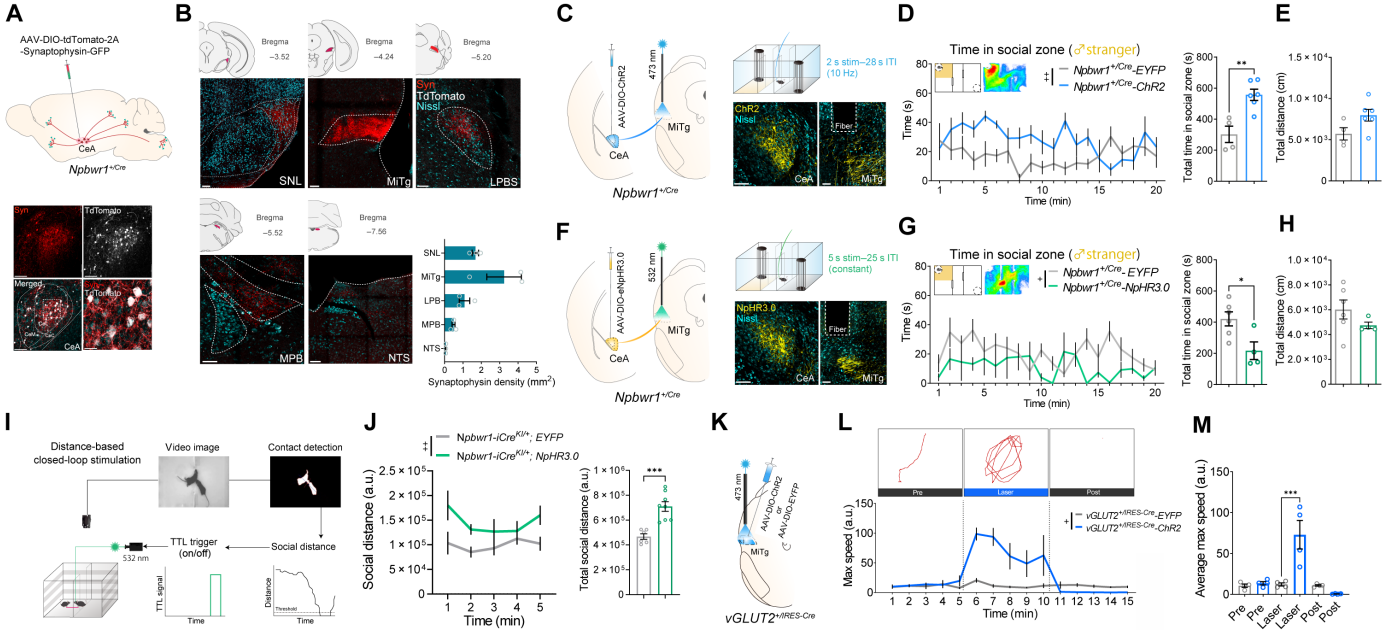

Fig. 3. CeA^{Npbwr1} neurons act on MiTg to change the social distance and behavior. (**A**) Experimental protocol for anterograde tracing. Bottom shows the expression of synaptophysin-GFP and tdTomato in the CeA. Bottom right shows a high-power view of the dotted rectangle region. Scale bar, 100 μm. (**B**) Expression of tdTomato and synaptophysin-GFP in the SNL, MiTg, LPBS (lateral parabrachial nucleus), MPB (medial parabrachial nucleus), and NTS (nucleus tractus solitarius). Scale bars,100 μm. Bar graph shows density of synaptophysin in designated brain regions. (**C**) Protocol for optogenetic excitation. Scale bars, 100 μm. (**D**) Left: Time spent in the social zone with optogenetic stimulation of CeA ^{Npbwr1} fibers in the MiTg. Right: Average time spent in the social zone. EYFP: $n = 4$; ChR2: $n = 6$. (**E**) Total distance during the three-chamber test with optogenetic stimulation. (**F**) Protocol for optogenetic inhibition. (**G**) Left: Time spent in the social zone with constant stimulation (EYFP: $n = 6$; eNpHR3.0: $n = 4$). Right: Average time in the social zone. (**H**) Total distance during the three-chamber test with optogenetic inhibition. (**I**) Experimental design for social contact-triggered feedback manipulation. (**J**) Left: Change in social distance (EYFP: $n = 6$; eNpHR3.0: $n = 8$). Right: Average change in total social distance. Values are represented as means ± SEM. (**K**) Optogenetic activation of vGLUT2 expressing neurons in MiTg induces fear-related response. Cre-dependent AAV driving ChR2-EYFP or EYFP was injected into the MiTg (*vGLUT2*$^{+/IRES\text{-}Cre}$). (**L**) Optogenetic excitation of vGLUT2-positive neurons in the MiTg. (**M**) Average maximum speed during the test session. Data are from *vGLUT2*$^{+/IRES\text{-}Cre}$ mice (ChR2: $n = 4$; EYFP: $n = 4$). Bar and line graphs represent mean ± SEM. $^{+}P < 0.05$, $^{++}P < 0.01$, $^{*}P < 0.05$, $^{**}P < 0.01$, and $^{***}P < 0.001$.

the time spent in the social zone without changing the total distance traveled during the test (Fig. 3, D and E). Likewise, optogenetic inhibition of CeA^{Npbwr1} fibers in MiTg decreased the time spent in the social zone without changing the total distance traveled during the test (Fig. 3, F to H).

To investigate whether the increased activity of CeA^{Npbwr1} fibers in the MiTg is essential for maintaining physical contact during social interactions, we developed a system using Bonsai (Fig. 3I) (*21*), which inhibits CeA^{Npbwr1} fibers in the MiTg at the time of physical contact, leading to an increase in social distance from unfamiliar mice. These observations suggest that CeA^{Npbwr1} neurons, at least partially, mediate increased sociability with unfamiliar mice by acting on the MiTg (Fig. 3J) and that their activity is necessary for sustaining physical contact with novel conspecifics. Furthermore, optogenetic excitation of excitatory MiTg neurons elicited a flight-like aversive response (Fig. 3, K to M). In summary, because CeA^{Npbwr1} neurons are GABAergic (*18*), they are activated upon recognizing novel conspecifics and inhibit MiTg neurons to mitigate risk management behavior when contacting unfamiliar individuals.

Excitation of CeA^{Npbwr1} neurons restores sociability deficits

Next, since CeA^{Npbwr1} neurons increases sociability, we examined whether their activation of CeA^{Npbwr1} neurons could effectively alleviate sociability impairments induced by CSDS (*23*). We first expressed hM3Dq-mCherry in the CeA^{Npbwr1} neurons of *Npbwr1*$^{+/Cre}$ mice. We then exposed them to a 10-min session of CSDS per day, consisting of encounters with CD-1 mice acting as aggressors, repeated over 7 days. Last, we conducted the social interaction test (SIT) to evaluate the effects of CSDS and select susceptible (SUS) mice. Subsequently, we performed a three-chamber social test and a social test (Fig. 4A). SUS mice showed decreased sociability with the novel CD-1 mice in the SIT; however, this tendency was not observed

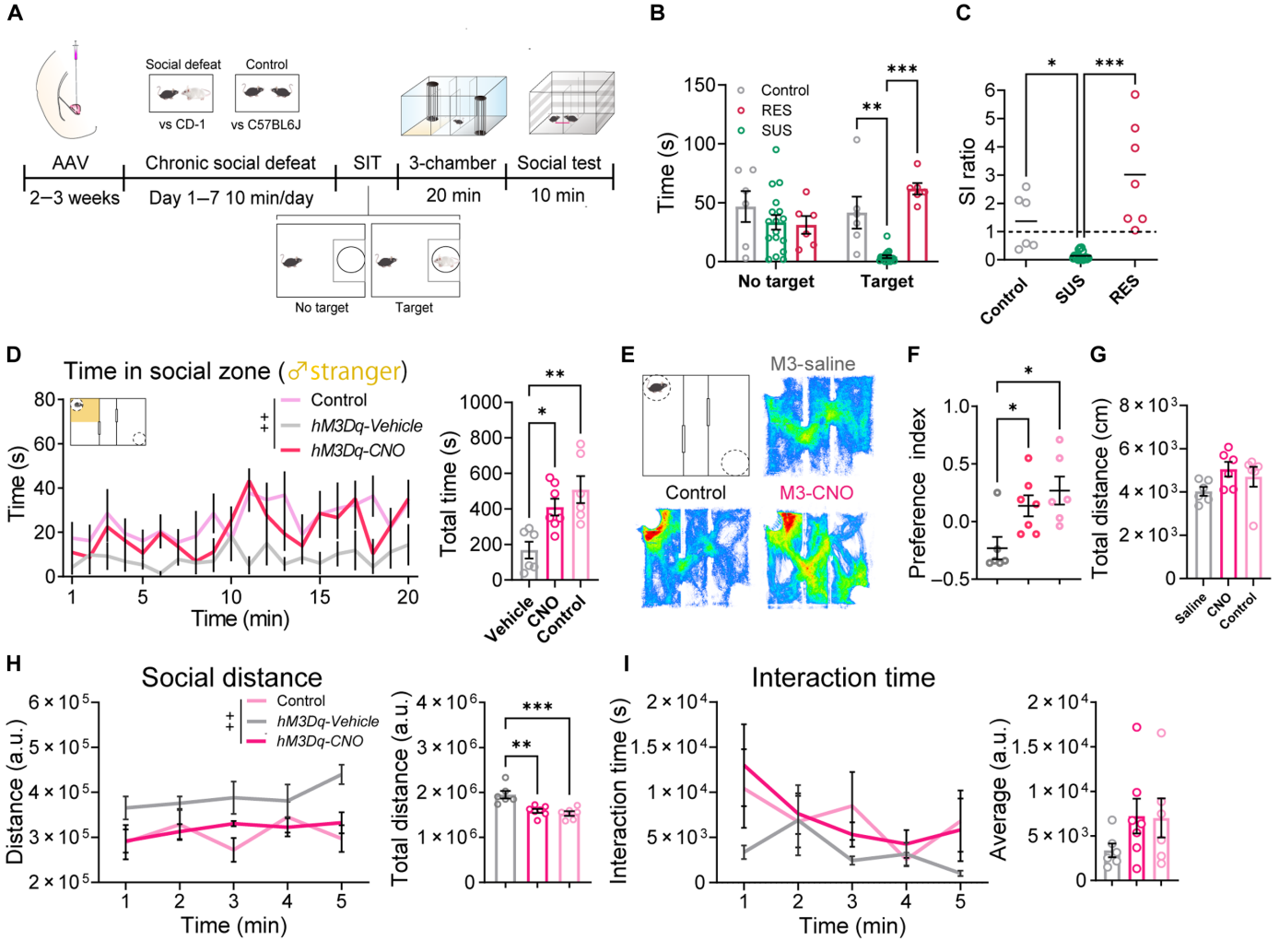

Fig. 4. Chemogenetic activation of CeA^{Npbwr1} neurons alters social behavior following CSDS. (**A**) Experimental schedule for DREADD experiments with CSDS. (**B**) Time spent in a zone with or without target (CD-1) (control: $n = 6$; SUS: $n = 17$; RES = 7). (**C**) Social interaction ratio (SI ratio) following CSDS. (**D**) Left: Time in the social zone in a three-chamber social test following chemogenetic activation of CeA^{Npbwr1} neurons. Right: Average time in the social zone. Vehicle: $n = 6$; CNO: $n = 7$; control = 6. (**E**) Heatmaps showing the time spent in the three-chamber social chamber. (**F**) Preference index is evaluated by calculating time spent in social and empty zones. (**G**) Total distance during the three-chamber test. (**H**) Left: Social distance change following chemogenetic activation. Right: Average social distance. (**I**) Left: Social interaction time. Right: Average social interaction time. For the entire figure, values are represented as means ± SEM. $^{++}P < 0.01$, two-way ANOVA with Sidak's multiple comparisons test; $^{*}P < 0.05$, $^{**}P < 0.01$, and $^{***}P < 0.001$, one-way ANOVA with Sidak's multiple comparisons test. Each dot is one mouse.

in resilient (RES) mice (Fig. 4, B and C). Sociability deficits with the novel C57B6J mice were also observed, which is consistent with a previous study (*24*). Mice expressing hM3Dq-mCherry in CeA^{Npbwr1} neurons after saline injection showed the same tendency (Fig. 4D). However, CNO administration in these mice markedly increased the time spent in the social zone with a novel conspecific to a level similar to that of the control group (Fig. 4, D to F). The total distance traveled did not differ between the groups (Fig. 4G). Social distance with a novel conspecific also decreased, but social interaction time did not change in the CNO injection group compared to the saline group (Fig. 4, H and I). These results suggest that the activation of CeA^{Npbwr1} neurons resulted in recovery from sociability deficits induced by CSDS, indicating that CeA^{Npbwr1} neurons could serve as a target for new therapeutics against sociability deficits.

NPBWR1 modulates the activity of CeA^{Npbwr1} neurons to regulate social behavior

To understand how NPBWR1 affects the function of CeA^{Npbwr1} neurons, we examined the activity of these neurons in *Npbwr1*$^{Cre/Cre}$ mice, which lack endogenous *Npbwr1* expression, with or without exogenous rescue of human *NPBWR1* expression. Since human NPBWR1 has a frequent SNP (404A>T, Y135F) in the coding region, which affects receptor functions due to reduced coupling with the Gi subclass of G proteins (*19*), we used both the wild-type *NPBWR1(135Y)* and the variant *NPBWR1(135F)* in this experiment. We injected *AAV-DIO-jRGECO1a* and Cre-dependent AAV carrying human *NPBWR1(135Y)-EYFP* or *NPBWR1(135F)-EYFP*. Red fluorescent signals were obtained from the optic fibers implanted in the CeA while monitoring the distance between the two mice (Fig. 5A). The activity of CeA^{Npbwr1} neurons expressing NPBWR1(135F) increased when the mice contacted novel conspecifics, displaying a pattern similar to that of the control group (*Npbwr1*$^{Cre/Cre}$) (Fig. 5, B and C). However, this change was significantly small in mice expressing NPBWR1(135Y). A similar change in differential activity was observed in female mice (fig. S8, B and C). Conversely, the activity of CeA^{Npbwr1} neurons expressing either NPBWR1(135F) or (135Y) showed no remarkable change when the mice started contacting cage mates (Fig. 5, D and E) or toy mice (fig. S8, D and E). NPBWR1(135Y) overexpression might block the increase in CeA^{Npbwr1} neuron's activity upon contacting strangers, presumably responding to endogenous ligands, NPB, and/or NPW.

Next, we examined how the expression of *NPBWR1(135Y)* or *NPBWR1(135F)* affects social behavior of *Npbwr1*$^{Cre/Cre}$ mice (Fig. 6A). *Npbwr1*$^{Cre/Cre}$ mice, which lack *Npbwr1* expression, stayed for a longer time in the social zone in the three-chamber social test than *Npbwr1*$^{+/Cre}$ mice, showing that the lack of NPBWR1 increased social contact with strangers (fig. S2, B and C). Exogenous expression of *NPBWR1(135Y)*, but not *NPBWR1(135F)*, decreased time in the social zone in the three-chamber social test (Fig. 6B). The tendency of *Npbwr1*$^{Cre/Cre}$ mice to go into the social zone more compared to the empty zone was abolished by *NPBWR1(135Y)* expression in CeA^{Npbwr1} neurons (Fig. 6C). The total distance traveled during the three-chamber test did not change (Fig. 6D). *NPBWR1(135Y)* expression also increased the social distance and decreased the number of contacts with male stranger conspecifics (Fig. 6, E and F). Thus, we concluded that the expression of *NPBWR1(135Y)* decreases the tendency to approach novel conspecifics when expressed in CeA^{Npbwr1} neurons, and the SNP(Y135F) abolished this effect. To further support this, microinjection of NPB into the CeA decreased

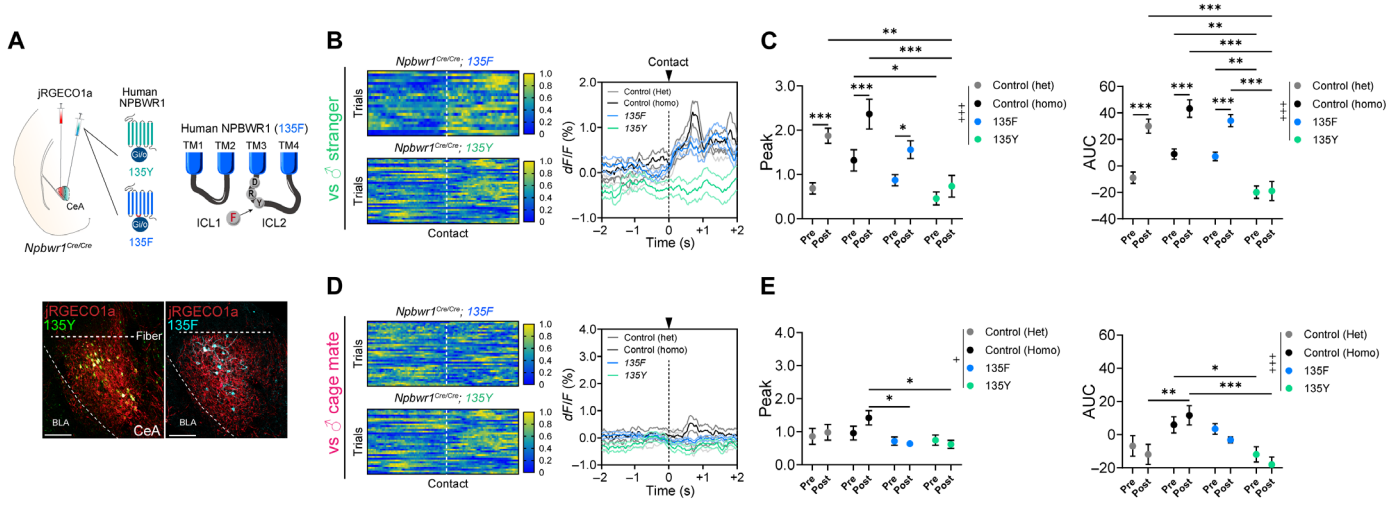

Fig. 5. NPBWR1 affects the activity of CeA^{Npbwr1} neurons. (**A**) Top: A schematic drawing of AAV and optic fiber implantation. The cartoon shows the localization of SNP in the structure of human NPBWR1. Bottom: Representative jRGECO1a and NPBWR1(135F) (left) and NPBWR1(135Y) (right) expression. Scale bars, 100 μm. (**B**) Left: Activity heat plot of CeA^{Npbwr1} neurons with 135F (top) or 135Y (bottom) 2-s time windows before and after contact with a male stranger WT mouse. Right: Trial-averaged *dF/F* Ca^{2+} time course of CeA^{Npbwr1} neurons with NPBWR1(135F) or NPBWR1(135Y) and control (*Npbwr1*$^{Cre/+}$ and *Npbwr1*$^{Cre/Cre}$). (**C**) Left: Averaged peak *dF/F* Ca^{2+} 2 s before and after contact with a male stranger. Right: The average AUC. Data are from the *Npbwr1*$^{Cre/Cre}$ mice expressing jRGECO1a ($n = 4$, versus male stranger, 135F, 23 events; 135Y, 28 events) and jGCaMP7c [$n = 4$, versus male stranger, control (homo), 31 events; control (het), 32 events] in CeA^{Npbwr1} neurons. (**D**) Left: Activity heat plot of CeA^{Npbwr1} neurons with NPBWR1(135F) (top) or NPBWR1(135Y) (bottom) for 2 s before and after contact with a male cage mate. Right: Trial-averaged *dF/F* Ca^{2+} time course of CeA^{Npbwr1} neurons with 135F or 135Y and control (*Npbwr1*$^{Cre/+}$ and *Npbwr1*$^{Cre/Cre}$). (**E**) Left: Averaged peak *dF/F* Ca^{2+} in 2 s before and after contact with a male cage mate. Right: The average AUC. Data are from the *Npbwr1*$^{Cre/Cre}$ mice expressing jRGECO1a ($n = 4$, versus cage mate, 135F, 37 events; 135Y, 34 events) and jGCaMP7c [$n = 4$, versus male stranger, control (homo), 31 events; control (het), 32 events] in CeA^{Npbwr1} neurons. Values are represented as means ± SEM. $^{+}P < 0.05$, $^{+++}P < 0.001$, $^{*}P < 0.05$, $^{**}P < 0.01$, and $^{***}P < 0.001$.

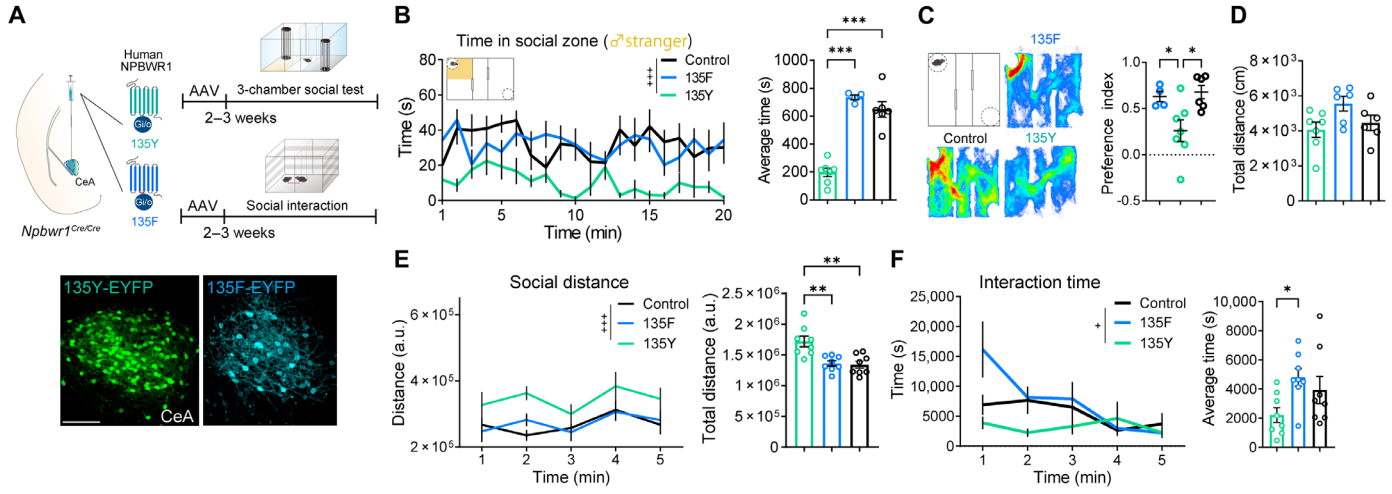

Fig. 6. NPBWR1 alters social distance and behavior. (**A**) Top: Rescue expression of *NPBWR1(135F)* or *NPBWR1(135Y)* in CeA^{Npbwr1} neurons in *Npbwr1*$^{Cre/Cre}$ mice for performing the three-chamber social test and SIT. Bottom: Expression of NPBWR1(135Y) (left) and NPBWR1(135F) (right). Scale bar, 100 μm. (**B**) Left: Time in the social zone in the three-chamber social test. Right: Average time in the social zone. (**C**) Heatmap shows the change of trajectory in the three-chamber test. Right: Preference index between NPBWR1(135Y)- and NPBWR1(135F)-expressing groups. Data are from the *Npbwr1*$^{Cre/Cre}$ mice (control, $n = 6$) and *Npbwr1*$^{Cre/Cre}$ mice expressing NPBWR1 (135Y, $n = 4$) and NPBWR1 (135F, $n = 7$). (**D**) Total distance during the three-chamber test in (B). (**E**) Change of social distance. (**F**) Interaction time. Data are from the *Npbwr1*$^{Cre/Cre}$ mice (control, $n = 8$) and *Npbwr1*$^{Cre/Cre}$ mice expressing NPBWR1 (135Y, $n = 8$) and NPBWR1 (135F, $n = 8$). For the entire figure, values are represented as means ± SEM. $^{+}P < 0.05$, $^{+++}P < 0.001$, two-way ANOVA with Sidak's multiple comparisons test; $^{*}P < 0.05$, $^{**}P < 0.01$, and $^{***}P < 0.001$, one-way ANOVA with Sidak's multiple comparisons test.

the time spent in the social zone and locomotor activity (fig. S9). These results suggest that the NPB/W-NPBWR1 system is a negative regulator of sociability, acting as an inhibitory mechanism for CeA^{Npbwr1} neurons, which increases social novelty preference, and that the SNP(Y135F) in human *NPBWR1* affects this function.

DISCUSSION

Creating new social interactions is essential for social animals; however, it concurrently presents inherent risks. Comprehension of the mechanisms governing the attainment of equilibrium between these dual facets, thereby enabling the enactment of suitable social behavior, remains limited. Disruption of this intricate mechanism may conceivably precipitate conditions such as sociophobia, as documented in previous studies (*25*, *26*). In addition, an excessive propensity toward familiarity can exacerbate social predicaments. These observations provide an understanding of the mechanisms by which novel social preferences are important in an era marked by a highly complex human society.

In our previous study, we observed that *Npbwr1*$^{-/-}$ mice displayed abnormal social behavior (*18*). These behaviors include impulsive interactions with unfamiliar mice, intensified approaches, extended periods of contact, and longer chasing durations. These findings highlight the importance of further investigation into the role of *Npbwr1*-expressing neurons in the preference for social novelty.

We demonstrated that CeA^{Npbwr1} neurons play a key role in regulating social novelty preference. Physical contact and withdrawal from social novelty increased and decreased the activity of CeA^{Npbwr1} neurons, respectively. CeA^{Npbwr1} neurons act on MiTg neurons to decrease social fear/anxiety-related behaviors and maintain physical contact. No change in the activity of CeA^{Npbwr1} neurons was observed upon encountering familiar mice (cage mates) (Fig. 1, E and F). This suggests that CeA^{Npbwr1} neurons exhibit different activity patterns, depending on whether the contacts are familiar or unfamiliar. Such differential regulation may be necessary for mice to manage novel social contacts that are associated with notable levels of anxiety.

CeA^{Npbwr1} neurons show increased activity immediately after physical contact with novel conspecifics. This suggests that these neurons respond to signals such as tactile information or nonvolatile pheromone signals. However, further research is needed to identify the molecular mechanism that determines whether an opponent is familiar or a stranger.

This study primarily focused on male mice interacting with unfamiliar male conspecifics and objects. However, as shown in fig. S4, the activation of CeA^{Npbwr1} neurons was consistent during interactions with both male and female unfamiliar mice. This suggests that the role of these neurons in processing social recognition may be conserved across encounters with both sexes and that CeA^{Npbwr1} neurons likely contribute similarly to responses involving unfamiliar female conspecifics. While our data did not include direct observations of female mice, further studies incorporating female-specific data, including female-female interactions, will be valuable to extend our findings to female social interactions.

The CeA acts as a hub, gating and modulating information from various inputs, which regulate appetitive and aversive motivated behaviors (*9*, *10*, *27*, *28*). Different modalities of social information altered the activity of CeA^{Npbwr1} neurons (Fig. 1 and fig. S4), suggesting that these neurons receive diverse inputs. Neurons that made direct synaptic contact with CeA^{Npbwr1} neurons were found in various brain regions (fig. S6). The pBLA, AmPir, and vCA1 comprised the primary input regions of CeA^{Npbwr1} neurons (fig. S9, C and D), suggesting that these input neurons play a role in differentially regulating CeA^{Npbwr1}

neurons depending on whether the contacts are novel or familiar. Given that AmPir and vCA1 have been implicated in odor-induced hormonal fear responses and social memory (*29*–*32*), these regions could be candidates that regulate CeA^{Npbwr1} neurons. In addition, given that tyrosine hydroxylase–positive neurons in the dorsal raphe express NPW and send abundant projections to the CeA, this input could be involved in regulating CeA^{Npbwr1} neuron activity (*33*).

Various gene markers have been identified in CeA neurons, indicating the functional diversity of the CeA (*27*, *34*). The expression of *Pkc*δ and *Som* suggests that CeA^{Npbwr1} neurons could function as a part of the mutual disinhibitory circuit in the CeA, regulating fear behavior (*14*, *15*). Future studies are needed to uncover the functional overlap between CeA^{Npbwr1} neurons and *Tac2/Nts* expressing CeA neurons, which have been reported to be involved both in fear and anxiety behaviors and sleep regulation (*35*, *36*).

We also showed that NPBWR1, a Gi protein–coupled inhibitory receptor, is a negative regulator of this pathway (Figs. 5 and 6). The SNP (404A>T) in *NPBWR1* showed functional impairment as a Gi protein–coupled receptor and correlated with differential emotional valence in human face recognition (*19*). Differential calcium dynamics of CeA^{Npbwr1} neurons overexpressing *NPBWR1(135F)* or *(135Y)* in *NPBWR1*$^{Cre/Cre}$ mice encountering unfamiliar mice (Fig. 5, B and C) further suggested that the SNP (404A>T) decreases receptor function. We also found that *NPBWR1(135F)* or *(135Y)* expression in CeA^{Npbwr1} neurons in *Npbwr*1-deficient *Npbwr1*$^{Cre/Cre}$ mice differentially alter social behavior (Fig. 6). This finding suggests the intriguing possibility that the SNP in human *NPBWR1* could be a contributing factor in determining individual differences in social behavior toward strangers.

Our findings suggested that activating CeA^{Npbwr1} neurons can rescue social interaction deficits observed after CSDS (Fig. 4). Notably, the lack of social interaction in these models may not necessarily be due to the direct dysfunction of CeA^{Npbwr1} neurons. As previously reported, social behavior deficits after CSDS may stem more from trauma-mediated avoidance than from impaired social recognition. While our study focused on demonstrating the efficacy of CeA^{Npbwr1} neuronal activation in improving social behavior, the underlying mechanisms responsible for these changes remain unclear. Further research is required to elucidate how CeA^{Npbwr1} neurons interact with broader neural circuits involved in social behavior, as well as how CSDS affects signaling. Future studies should investigate these mechanisms in greater detail, including the potential development of interventions targeting CeA^{Npbwr1} neuronal control systems to mitigate social deficits.

The NPB/W-NPBWR1 system potentially assumes the role of a negative regulatory entity within this pathway, contributing to the preservation of appropriate interindividual distancing from unfamiliar individuals, thereby respecting the boundaries of the personal space of others. NPB injection into the CeA decreased sociability toward unfamiliar individuals (fig. S9). An SNP (404A>T) found in the human *NPBWR1* gene also affects the function of this mechanism (Fig. 6), raising the intriguing possibility that this SNP influences social-behavioral characteristics in humans (*19*). This is supported by previous reports showing that this SNP correlates with psychological differences in humans when presented with the various emotional faces of others (*19*). Furthermore, humans have the NPB/W receptor subtype NPBWR2, which is absent in rodents, suggesting that this receptor may have evolved to handle the complex social interactions observed in human society. If agonists or antagonists of NPBWRs are developed, then they can influence human behavioral tendencies toward others and social behavior. These pharmacotherapeutics may be beneficial for treating social phobia and disinhibiting social engagement disorders (*37*).

MATERIALS AND METHODS

Animals

All animal experiments were performed at the International Institute for Integrative Sleep Medicine (IIIS), Tsukuba University, according to the guidelines for animal experiments. The experiments were approved by the Animal Experiment Committee (24-065) and were in accordance with the National Institutes of Health guidelines. Mice were given food and water ad libitum and maintained at 23°C, relative humidity of 50%, with a 12-hour light/12-hour dark cycle. Adult male mice (10 to 14 weeks old) were used in all experimental procedures except for 16- to 24-month-old male CD-1(ICR) mice (sexually experienced retired breeders; the Jackson Laboratory). All mice used in this study, including wild-type [C57BL/6J male mice (ID# 000664 from Charles River)] and transgenic mice, were bred at the IIIS, except for male CD-1(ICR) mice. The experimental mice were cohoused with male wild-type mice as cage mates. Group-housed male wild-type mice were used for all behavioral tests, and female wild-type mice were used as strangers for fiber photometry experiments. *Npbwr1*$^{+/Cre}$ mice were generated by homologous recombination of C57/BL6N embryonic stem cells, followed by the implantation of eight–cell stage embryos (fig. S1).

Viruses

AAVs were produced using a triple-transfection helper-free method, as described previously (*38*). The final purified viruses were stored at −80°C. Titers of recombinant AAV vectors were determined by quantitative polymerase chain reaction: *AAV*$_{10}$*-EF1*α*-DIO-hM3Dq-mCherry*; *AAV*$_{10}$*-EF1*α*-DIO-hM4Di-mCherry*; 1.90×10^{12}, *AAV*$_{10}$*-EF1*α*-DIO-TVA-mCherry*; 4×10^{13}, *AAV*$_{10}$*-CAG-DIO-RG*; 3.9×10^{13}, *AAV*$_{10}$*-EF1*α*-DIO-ChR2-EYFP*; 3.7×10^{13}, *AAV*$_{10}$*-EF1*α*-DIO-EYFP*; 5.82×10^{13}, *AAV*$_{10}$*-hsyn-DIO-mCherry*; 2.6×10^{13}, *AAV*$_{10}$*-hsyn-DIO-jGCaMP7c*; 5.03×10^{13}, *AAV*$_{10}$*-hsyn-DIO-GCaMP6s*; 4.2×10^{13}, *AAV*$_{2/9}$*-hsyn-DIO-tdTomato-T2A-synaptophysin-EGFP*; 2.5×10^{13}, *AAV*$_{2}$*-EF1*α*-DIO-NPBWR1(135F)-EYFP*; 1.82×10^{13}, *AAV*$_{2}$*-EF1*α*-DIO-NPBWR1(135Y)-EYFP*; 7.04×10^{12} genome copies/ml. We made *SAD*△*G-GFP* (EnvA) by transfecting these plasmids in B7GG cells, followed by pseudotyping in BHK-RGCD-EnvA cells and ultracentrifugation (*39*); 4.2×10^{13} infectious units/ml.

Surgery

For the injection of AAV vectors, male *Npbwr1*$^{Cre/Cre}$ or *Npbwr1*$^{+/Cre}$ mice (10 to 12 weeks old) were anesthetized with isoflurane (Pfizer) and positioned in a stereotaxic frame (David Kopf Instruments). For fiber photometry, we injected *AAV*$_{10}$*-hsyn-DIO-jGCaMP7c*, *AAV*$_{10}$*-hsyn-DIO-GCaMP6s*, *AAV*$_{2/9}$*-hsyn-DIO-jRGECO1a*, *AAV*$_{10}$*-EF1*α*-mCherry*, *AAV*$_{10}$*-EF1*α*-NPBWR1(135F)-EYFP*, and *AAV*$_{10}$*-EF1*α*-NPBWR1(135Y)-EYFP* into the CeA [anterior-posterior (AP), −1.48 mm; medial-lateral (ML), +3.05; dorso-ventral (DV), −4.45 mm from the bregma; 0.3 to 0.4 μl]. Optical fiber was implanted above the CeA [(AP), −1.48 mm; (ML), +3.05; (DV), −4.38]. For chemogenetic manipulation, we injected *AAV*$_{10}$*-EF1*α*-DIO-hM3q-mCherry* and *AAV*$_{10}$*-EF1*α*-DIO-hM4Di-mCherry* into the CeA. For anterograde tracing, we injected *AAV*$_{2/9}$*-hsyn-DIO-tdTomato-T2A-synaptophysin-EGFP* into the CeA.

For retrograde tracing, we injected *AAV_{10}-EF1α-DIO-TVA-mCherry*, *AAV_{10}-EF1α-DIO-RG*, and *SADΔG-GFP* into the CeA. For optogenetic manipulation, we injected *AAV_{10}-EF1α-DIO-ChR2-EYFP* and *AAV_{10}-EF1α-DIO-eNpHR3.0-EYFP* into the CeA. Then, optical fibers were implanted above MiTg (AP, −4.2 mm; ML, ±1.8 mm; DV, −3.23 mm). Behavioral experiments were performed 2 to 3 weeks after virus injection. For microinjection into the CeA, cannulae were implanted bilaterally above the CeA. Behavioral experiments were performed 1 week after implantation.

Drug administration

CNO (Abcam, ab141704) was dissolved in saline at a dose of 100 μg/ml and frozen at −20°C. CNO was administered intraperitoneally at a dose of 5 mg/kg. NPB (NPB-29, rat, 4459-v, Peptide Institute) was injected at a dose of 10 nM into the CeA. NPB was diluted in ddH_2O (double-distilled water) up to 1 μM and then diluted with artificial cerebrospinal fluid (R&D Systems), which also used as a control.

Behavior tests

All behavioral tests were performed under dim light conditions (<15 lx) using two- and three-compartment arenas with a charge-coupled device (CCD) video camera to record social distance and behavior. The experimental mice were cohoused with male wild-type mice after surgery.

Three-chamber social test

For the three-chamber social test, mice were habituated to a three-compartment experimental arena (40 cm by 52 cm by 25 cm, acrylic glass), which was divided into three rooms (center: 40 cm by 12 cm by 25 cm, left and right: 40 cm by 20 cm by 25 cm) with two empty cylindrical cages inside with removable doors (fig. S2A). To evaluate sociability, the mice were placed in the center of the arena, separated by two doors for 5 min, after habituation without these doors for 20 min. A male stranger mouse (C57/BL6J, 10 to 14 weeks old) was placed in one of the cylindrical cages. A different stranger male mouse was used for each session. After 3 min, the doors were removed for 20 min to record social behavior. To evaluate social novelty preference, we placed a male stranger mouse and a cage-mate mouse in each cylindrical cage for 10 min after habituation without these mice. Notably, the stranger mice used in both tests were of the same sex and age as the test mice. The preference index (%) was calculated as the time spent exploring strangers subtracted from the time spent exploring empty or cage mates, divided by the total time spent with both subjects. The behavior of the mice was recorded with a CCD video camera, and the time spent around the cylindrical cages was analyzed using SMART 3.0 (Panlab) software.

Social interaction test

The experimental mice and male stranger wild-type mice (C57/BL6J, 10 to 14 weeks old) were placed in a two-compartment experimental arena (40 cm by 40 cm by 25 cm, acrylic glass) divided into two rooms (left and right; 40 cm by 20 cm by 25 cm), with a door in the middle (fig. S2F). After 5 min of habituation, the door was opened for 5 min to analyze the social distancing and behavior. A different stranger male mouse was used for each session. The behavior of the mice was recorded with a CCD video camera, and social behavior and distance were analyzed using Bonsai software running a Python-based custom-made algorithm (*21*, *40*).

Elevated plus maze

An experimental mouse was placed in the center zone of an elevated plus maze apparatus (both open and closed arms were 40 cm in length). A 5-min video recording was conducted immediately after placing the mouse in the center. The behavior of the mice was analyzed using an automated software (SMART 3.0, Panlab).

Chronic social defeat stress

CSDS was performed as previously described (*23*). A single experimental mouse was exposed to a different CD-1 aggressor mouse for 10 min each day for seven consecutive days. The severity of aggressive attacks in CD-1 mice was screened before the CSDS procedure to maintain the homogeneity of aggression of CD-1 mice. After each 10-min contact, a group-housed experimental mouse was moved to a different cage where a single CD-1 mouse stayed. As a control, group-housed *$Npbwr1^{+/Cre}$* mice were exposed to a different home cage than the C57BL6J mice. On day 8, defeated and control animals were subjected to a SIT, with or without CD-1. The social interaction ratio was calculated as the time spent exploring the CD-1 mice divided by the time spent exploring the empty cage. Only SUS animals scoring <1, as evaluated by the SIT, were used for further behavioral analysis.

Optogenetic manipulation

We used a 473- or 532-nm laser (Shanghai Laser & Optics Century Co. Ltd.) connected to patch cords [200-μm diameter; numerical aperture (NA): 0.22, 1.0 m long; Doric Lenses], a rotary joint (Doric Lenses), and a ferule-attached optic cannula (200-μm diameter; NA: 0.5, 6 mm long; Kyocera). The laser intensity was calibrated from 5 mW at the fiber tip using a power meter (Coherent Corp) and estimated using a light transmission calculator (https://web.stanford.edu/group/dlab/cgi-bin/graph/chart.php) before initiating the behavioral experiments.

For the excitation of MiTg-projecting CeA^{Npbwr1} neurons, we repeatedly performed 2 s of photostimulation at 28-s intervals for 20 min in the three-chamber test. To inhibit these neurons, we repeatedly performed 5-s photostimulation at 25-s intervals for 20 min in the three-chamber test. During preliminary experiments, we found that the stimulation parameters used were sufficient to produce the desired effects and avoid the risks of tissue damage and photobleaching of opsin during the experimental period.

For the social distance–dependent feedback inhibition of MiTg-projecting CeA^{Npbwr1}neurons, we combined Bonsai with Arduino (Arduino Uno, Arduino) to transform social contact information (social distance is zero) into TTL signals. A 532-nm laser was controlled by TTL signals to stimulate constantly only when the social distance became zero.

Immunohistochemistry

Mice were anesthetized with sodium pentobarbital and then fixed by intracardiac perfusion with 4% paraformaldehyde. Then, the brains were postfixed for 24 hours in the same fixative and cryoprotected by immersion in 30% sucrose for 2 days. Brain sections of 40-μm thickness were cut with a cryostat. Sections were incubated with 1% Triton X-100 in phosphate-buffered saline (PBS) for 1 hour, and then incubated and blocked with 10% bovine serum albumin (Blocking One, Nacalai Tesque) and 0.3% Triton X-100 in PBS for 1 hour. Then, slices were incubated with the designated primary antibodies in PBS overnight at 4°C. The slices were washed with PBS containing 0.25% Triton

X-100 and 3% bovine serum albumin. Then, slices were incubated with the designated primary antibodies in PBS overnight at 4°C. Rabbit polyclonal antibodies against rat anti-cFos (1:5000; Ab-5, Millipore), mouse anti-tyrosine hydroxylase (1:2500; F-11, Santa Cruz), and goat anti-GFP (1:1000; Molecular Probes) were used. Then, slices were washed with PBS three times, followed by incubation with the designated secondary antibodies in PBS for 2.5 hours. Secondary antibodies used in this study were Alexa Fluor 594–conjugated donkey anti-rabbit, 594-conjugated donkey anti-mouse, 488-conjugated donkey anti-mouse, and 488-conjugated donkey anti-rabbit (1:1000; Molecular Probes, Eugene, OR). The slices were washed three times in PBS, mounted on subbed slides, air-dried, and covered with coverslips using a reagent (Fluor Save, Calbiochem). The brain sections were observed using a confocal laser microscope (SP8, Leica) and a microscope (Axio Zoom V16, Zeiss).

In situ hybridization

Fluorescence in situ hybridization was performed using an RNAscope Fluorescent Multiplex Kit (Advanced Cell Diagnostics) with the following probes: Probe-Mm-*CRH*-316091-C2, Mm-*Npbwr1*–840781-C1, Mm-*NTS*-420441-C2, Mm-*PRKCD*-441791-C2, Mm-*SST*-404631-C3, and Mm-*Tac2*–446391-C3.

Mice were perfused and fixed using the same procedure as described in the "Immunohistochemistry" section except using diethyl pyrocarbonate–treated PBS and 4% paraformaldehyde. Brains were sectioned coronally into sections (20 μm) with a cryostat (Leica) and mounted on slides (Superfrost Plus Microscope Slides, Fisherbrand).

Retrograde tracing

For retrograde tracing, we injected viruses as shown below into the CeA of *Npbwr1*$^{+/Cre}$ mice. First, a cocktail of *AAV*$_{10}$*-DIO-TVA-mCherry* with *AAV*$_{10}$*-DIO-RG* (1:2) was delivered unilaterally to express TVA-mCherry and rabies glycoprotein in CeA^{Npbwr1} neurons (AP, −1.48 mm; ML, 3.05 mm; DV, 4.45 mm from the bregma). Two weeks later, *SADΔG-GFP (EnvA)* was injected at the same location. Six days later, mice were perfused and treated according to the procedure described in the "Immunohistochemistry" section. Starter (GFP and mCherry double positive) and input neurons (GFP positive) were observed in whole-brain sections using laser microscopes (Axiozoom.V16, Zeiss; TCS SP8, Leica).

Anterograde tracing

For anterograde tracing, we injected *AAV*$_{2/9}$*-hsyn-DIO-tdTomato-T2A-synaptophysin-EGFP* into the CeA of *Npbwr1*$^{+/Cre}$ mice. CeA^{Npbwr1} neurons (mCherry-positive) and their presynaptic synaptophysin signals (GFP) were observed in specific brain regions using a confocal laser microscope (TCS SP8, Leica). We quantified the GFP-positive synaptophysin density in each brain area [SNL, MiTg, lateral parabrachial nucleus (LPBS), superior part of the lateral parabrachial nucleus, medial parabrachial nucleus (MPB), and nucleus of the solitary tract (NTS)] using ImageJ software (*41*). A boxed area (150 μm by 150 μm) for the GFP channel of each brain region was cropped, converted to an eight-bit image, and binarized by thresholding. The threshold value for capturing synaptophysin signals in the medial prefrontal cortex of each mouse was manually determined. The threshold value was kept constant for all brain sections. The area fraction above the threshold was measured in each region, and the synaptophysin density in each region was calculated for each mouse.

Fiber photometry

We used a fiber photometry setup including a 465-nm light-emitting diode (LED) (CLED 465 nm, Doric Lenses) and a 560-nm LED (CLED 560 nm, Doric Lenses) for fluorophore excitation. Both LEDs were modulated at 1.2 kHz (465 and 560 nm) and controlled by a fiber photometry console (Doric Lenses) via an LED driver (Doric Lenses). The emission signal from the 465 nm excitation was collected via a patch cable (Thorlabs) connected to photodetectors (four-port fluorescence mini cube, Doric Lenses). The LED power was adjusted at the tip of the optical fiber to around 30 to 50 μW. A ferrule patch cord was connected to the ferrule fiber implanted in the subject mouse using a zirconia split sleeve (Kyocera). Recordings were initiated using Doric Neuroscience Studio (Doric Lenses) to control the photometry setup and camera (behavioral tracking camera, Doric Lenses). Signals were recorded in the lock-in demodulation mode at a sampling rate of 12.0 k/s decimated by a factor of 100 and saved as a comma-separated csv file (*42*). mCherry fluorescence intensity was used as an internal control to correct for variations in fluorescence levels. The values of fluorescence change (*dF/F*) were derived by calculating $(F_t - F_0)/F_0$, where F_0 is the baseline fluorescence signal calculated with the least mean square fit of the whole data series in each session. *dF/F* values are presented as means ± SEM.

Statistical analysis

All results are expressed as means ± SEM. Differences between individuals were analyzed using Spearman's rank correlation, two-tailed Student's *t* test, or one-way and two-way, analysis of variance (ANOVA), followed by Sidak's post hoc comparison analysis.

Supplementary Materials

The PDF file includes:

Figs. S1 to S9
Legend for movie S1
Table S1
References

Other Supplementary Material for this manuscript includes the following:

Movie S1

REFERENCES AND NOTES

1. S. Netser, A. Meyer, H. Magalnik, A. Zylbertal, S. H. de la Zerda, M. Briller, A. Bizer, V. Grinevich, S. Wagner, Distinct dynamics of social motivation drive differential social behavior in laboratory rat and mouse strains. *Nat. Commun.* **11**, 5908 (2020).
2. S. S. Moy, J. J. Nadler, A. Perez, R. P. Barbaro, J. M. Johns, T. R. Magnuson, J. Piven, J. N. Crawley, Sociability and preference for social novelty in five inbred strains: An approach to assess autistic-like behavior in mice. *Genes Brain Behav.* **3**, 287–302 (2004).
3. R. M. Hirschfeld, S. A. Montgomery, M. B. Keller, S. Kasper, A. F. Schatzberg, H. J. Möller, D. Healy, D. Baldwin, M. Humble, M. Versiani, R. Montenegro, M. Bourgeois, Social functioning in depression: A review. *J. Clin. Psychiatry* **61**, 268–275 (2000).
4. B. Barak, G. Feng, Neurobiology of social behavior abnormalities in autism and Williams syndrome. *Nat. Neurosci.* **19**, 647–655 (2016).
5. S. S. Moy, J. J. Nadler, N. B. Young, R. J. Nonneman, A. W. Grossman, D. L. Murphy, A. J. D'Ercole, J. N. Crawley, T. R. Magnuson, J. M. Lauder, Social approach in genetically engineered mouse lines relevant to autism. *Genes Brain Behav.* **8**, 129–142 (2009).
6. K. A. Stedenfeld, S. M. Clinton, I. A. Kerman, H. Akil, S. J. Watson, A. F. Sved, Novelty-seeking behavior predicts vulnerability in a rodent model of depression. *Physiol. Behav.* **103**, 210–216 (2011).
7. H. C. Breiter, N. L. Etcoff, P. J. Whalen, W. A. Kennedy, S. L. Rauch, R. L. Buckner, M. M. Strauss, S. E. Hyman, B. R. Rosen, Response and habituation of the human amygdala during visual processing of facial expression. *Neuron* **17**, 875–887 (1996).
8. P. J. Whalen, S. L. Rauch, N. L. Etcoff, S. C. McInerney, M. B. Lee, M. A. Jenike, Masked presentations of emotional facial expressions modulate amygdala activity without explicit knowledge. *J. Neurosci.* **18**, 411–418 (1998).

9. E. E. Steinberg, F. Gore, B. D. Heifets, M. D. Taylor, Z. C. Norville, K. T. Beier, C. Földy, T. N. Lerner, L. Luo, K. Deisseroth, R. C. Malenka, Amygdala-midbrain connections modulate appetitive and aversive learning. *Neuron* **106**, 1026–1043.e9 (2020).
10. E. Knapska, G. Walasek, E. Nikolaev, F. Neuhäusser-Wespy, H.-P. Lipp, L. Kaczmarek, T. Werka, Differential involvement of the central amygdala in appetitive versus aversive learning. *Learn. Mem.* **13**, 192–200 (2006).
11. A. Beyeler, P. Namburi, G. F. Glober, C. Simonnet, G. G. Calhoon, G. F. Conyers, R. Luck, C. P. Wildes, K. M. Tye, Divergent routing of positive and negative information from the amygdala during memory retrieval. *Neuron* **90**, 348–361 (2016).
12. S.-C. Lee, A. Amir, D. Haufler, D. Pare, Differential recruitment of competing valence-related amygdala networks during anxiety. *Neuron* **96**, 81–88.e5 (2017).
13. D. P. Kennedy, J. Gläscher, J. M. Tyszka, R. Adolphs, Personal space regulation by the human amygdala. *Nat. Neurosci.* **12**, 1226–1227 (2009).
14. S. Ciocchi, C. Herry, F. Grenier, S. B. E. Wolff, J. J. Letzkus, I. Vlachos, I. Ehrlich, R. Sprengel, K. Deisseroth, M. B. Stadler, C. Müller, A. Lüthi, Encoding of conditioned fear in central amygdala inhibitory circuits. *Nature* **468**, 277–282 (2010).
15. W. Haubensak, P. S. Kunwar, H. Cai, S. Ciocchi, N. R. Wall, R. Ponnusamy, J. Biag, H. W. Dong, K. Deisseroth, E. M. Callaway, M. S. Fanselow, A. Luthi, D. J. Anderson, Genetic dissection of an amygdala microcircuit that gates conditioned fear. *Nature* **468**, 270–276 (2010).
16. H. Li, M. A. Penzo, H. Taniguchi, C. D. Kopec, Z. J. Huang, B. Li, Experience-dependent modification of a central amygdala fear circuit. *Nat. Neurosci.* **16**, 332–339 (2013).
17. D. Viviani, A. Charlet, E. van den Burg, C. Robinet, N. Hurni, M. Abatis, F. Magara, R. Stoop, Oxytocin selectively gates fear responses through distinct outputs from the central amygdala. *Science* **333**, 104–107 (2011).
18. R. Nagata-Kuroiwa, N. Furutani, J. Hara, M. Hondo, M. Ishii, T. Abe, M. Mieda, N. Tsujino, T. Motoike, Y. Yanagawa, T. Kuwaki, M. Yamamoto, M. Yanagisawa, T. Sakurai, Critical role of neuropeptides B/W receptor 1 signaling in social behavior and fear memory. *PLOS ONE* **6**, e16972 (2011).
19. N. Watanabe, M. Wada, Y. Irukayama-Tomobe, Y. Ogata, N. Tsujino, M. Suzuki, N. Furutani, T. Sakurai, M. Yamamoto, A single nucleotide polymorphism of the neuropeptide B/W receptor-1 gene influences the evaluation of facial expressions. *PLOS ONE* **7**, e35390 (2012).
20. P. Tovote, J. P. Fadok, A. Lüthi, Neuronal circuits for fear and anxiety. *Nat. Rev. Neurosci.* **16**, 317–331 (2015).
21. G. Lopes, N. Bonacchi, J. Frazão, J. P. Neto, B. V. Atallah, S. Soares, L. Moreira, S. Matias, P. M. Itskov, P. A. Correia, R. E. Medina, L. Calcaterra, E. Dreosti, J. J. Paton, A. R. Kampff, Bonsai: An event-based framework for processing and controlling data streams. *Front. Neuroinform.* **9**, 7 (2015).
22. S. W. Oh, J. A. Harris, L. Ng, B. Winslow, N. Cain, S. Mihalas, Q. Wang, C. Lau, L. Kuan, A. M. Henry, M. T. Mortrud, B. Ouellette, T. N. Nguyen, S. A. Sorensen, C. R. Slaughterbeck, W. Wakeman, Y. Li, D. Feng, A. Ho, E. Nicholas, K. E. Hirokawa, P. Bohn, K. M. Joines, H. Peng, M. J. Hawrylycz, J. W. Phillips, J. G. Hohmann, P. Wohnoutka, C. R. Gerfen, C. Koch, A. Bernard, C. Dang, A. R. Jones, H. Zeng, A mesoscale connectome of the mouse brain. *Nature* **508**, 207–214 (2014).
23. S. A. Golden, H. E. Covington III, O. Berton, S. J. Russo, A standardized protocol for repeated social defeat stress in mice. *Nat. Protoc.* **6**, 1183–1191 (2011).
24. Y. Liu, S.-L. Deng, L.-X. Li, Z.-X. Zhou, Q. Lv, Z.-Y. Wang, F. Wang, J.-G. Chen, A circuit from dorsal hippocampal CA3 to parvafox nucleus mediates chronic social defeat stress–induced deficits in preference for social novelty. *Sci. Adv.* **8**, eabe8828 (2022).
25. Y. Hamasaki, N. Pionnié-Dax, G. Dorard, N. Tajan, T. Hikida, Preliminary study of the social withdrawal (hikikomori) spectrum in French adolescents: Focusing on the differences in pathology and related factors compared with Japanese adolescents. *BMC Psychiatry* **22**, 477 (2022).
26. M.-J. Guedj-Bourdiau, Claustration à domicile de l'adolescent Hikikomori. *Ann. Med. Psychol.* **169**, 668–673 (2011).
27. J. Kim, X. Zhang, S. Muralidhar, S. A. LeBlanc, S. Tonegawa, Basolateral to central amygdala neural circuits for appetitive behaviors. *Neuron* **93**, 1464–1479.e5 (2017).
28. H. Cai, W. Haubensak, T. E. Anthony, D. J. Anderson, Central amygdala PKC-δ+ neurons mediate the influence of multiple anorexigenic signals. *Nat. Neurosci.* **17**, 1240–1248 (2014).
29. K. Tao, M. Chung, A. Watarai, Z. Huang, M.-Y. Wang, T. Okuyama, Disrupted social memory ensembles in the ventral hippocampus underlie social amnesia in autism-associated Shank3 mutant mice. *Mol. Psychiatry* **27**, 2095–2105 (2022).
30. T. Okuyama, T. Kitamura, D. S. Roy, S. Itohara, S. Tonegawa, Ventral CA1 neurons store social memory. *Science* **353**, 1536–1541 (2016).
31. J. Lopez-Rojas, C. A. de Solis, F. Leroy, E. R. Kandel, S. A. Siegelbaum, A direct lateral entorhinal cortex to hippocampal CA2 circuit conveys social information required for social memory. *Neuron* **110**, 1559–1572.e4 (2022).
32. K. Kondoh, Z. Lu, X. Ye, D. P. Olson, B. B. Lowell, L. B. Buck, A specific area of olfactory cortex involved in stress hormone responses to predator odours. *Nature* **532**, 103–106 (2016).
33. T. Motoike, J. M. Long, H. Tanaka, C. M. Sinton, A. Skach, S. C. Williams, R. E. Hammer, T. Sakurai, M. Yanagisawa, O. Civelli, K. Kangawa, Mesolimbic neuropeptide W coordinates stress responses under novel environments. *Proc. Natl. Acad. Sci. U.S.A.* **113**, 6023–6028 (2016).
34. T. P. O'Leary, R. M. Kendrick, B. N. Bristow, K. E. Sullivan, L. Wang, J. Clements, A. L. Lemire, M. S. Cembrowski, Neuronal cell types, projections, and spatial organization of the central amygdala. *iScience* **25**, 105497 (2022).
35. M. Zelikowsky, M. Hui, T. Karigo, V. Gradinaru, B. E. Deverman, D. J. Anderson, A. Choe, B. Yang, M. R. Blanco, K. Beadle, The neuropeptide Tac2 controls a distributed brain state induced by chronic social isolation stress. *Cell* **173**, 1265–1279.e19 (2018).
36. C. Ma, P. Zhong, D. Liu, Z. K. Barger, L. Zhou, W.-C. Chang, B. Kim, Y. Dan, Sleep regulation by neurotensinergic neurons in a thalamo-amygdala circuit. *Neuron* **103**, 323–334.e7 (2019).
37. C. H. Zeanah, T. Chesher, N. W. Boris, American Academy of Child and Adolescent Psychiatry (AACAP) Committee on Quality Issues (CQI), practice parameter for the assessment and treatment of children and adolescents with reactive attachment disorder and disinhibited social engagement isorder. *J. Am. Acad. Child Adolesc. Psychiatry* **55**, 990–1003 (2016).
38. M. Mieda, D. Ono, E. Hasegawa, H. Okamoto, K.-I. Honma, S. Honma, T. Sakurai, Cellular clocks in AVP neurons of the SCN are critical for interneuronal coupling regulating circadian behavior rhythm. *Neuron* **85**, 1103–1116 (2015).
39. F. Osakada, E. M. Callaway, Design and generation of recombinant rabies virus vectors. *Nat. Protoc.* **8**, 1583–1601 (2013).
40. K. Sakurai, S. Zhao, J. Takatoh, E. Rodriguez, J. Lu, A. D. Leavitt, M. Fu, B.-X. Han, F. Wang, Capturing and manipulating activated neuronal ensembles with CANE delineates a hypothalamic social-fear circuit. *Neuron* **92**, 739–753 (2016).
41. C. A. Schneider, W. S. Rasband, K. W. Eliceiri, NIH Image to ImageJ: 25 years of image analysis. *Nat. Methods* **9**, 671–675 (2012).
42. R. B. Crouse, K. Kim, H. M. Batchelor, E. M. Girardi, R. Kamaletdinova, J. Chan, P. Rajebhosale, S. T. Pittenger, L. W. Role, D. A. Talmage, M. Jing, Y. Li, X.-B. Gao, Y. S. Mineur, M. R. Picciotto, Acetylcholine is released in the basolateral amygdala in response to predictors of reward and enhances the learning of cue-reward contingency. *eLife* **9**, e57335 (2020).
43. T. Takeuchi, T. Nomura, M. Tsujita, M. Suzuki, T. Fuse, H. Mori, M. Mishina, Flp recombinase transgenic mice of C57BL/6 strain for conditional gene targeting. *Biochem. Biophys. Res. Commun.* **293**, 953–957 (2002).

Acknowledgments: We thank J. Hara for preparing the AAV vectors. All plasmids used in this study were provided under material transfer agreements: pAAV-hsyn-DIO-GCaMP6s-WPRE-SV40 and pGP-AAV-syn-jGaMP7c from D. Kim, pAAV-EF1α-DIO-ChR2-EYFP-WPRE-HGHpA from K. Deisseroth, and pAAV-hSyn-DIO-tdTomato-T2A-SynaptophysinEGFP-WPRE from H. Zeng. **Funding:** This study was supported by a JSPS KAKENHI Grant-in-Aid for Scientific Research (B) (JP18H02595 to T.S. and JP21H02660 to S.S.), a KAKENHI Grant-in-Aid for Scientific Research on Innovative Areas, "Willdynamics" (16H06401), JSPS KAKENHI grant number JP19K22465 (to T.S.) and 23H04661 (to S.S), JSPS Fund for the Promotion of Joint International Research grant number 22K21351 (to T.S.), JST CREST grant number JPMJCR1655 Japan (to T.S.), Japan Foundation for Applied Enzymology (to S.S), Naito Foundation (to S.S.), Senri Life Science Foundation (to S.S), Takeda Science Foundation (to S.S), Uehara Memorial Foundation (to S.S. and T.S.), Grant-in Scientific Research on Innovation Areas "Integrative Research towards Elucidation of Generative Brain Systems for Individuality" (19H04894) (to S.S.), and AMED grant number JP21zf0127005 (to T.S.). **Author contributions:** S.S. and T. S. conceived the project and designed the experiments. S.S. performed all the experiments. S.S. and K.T. analyzed the photometric data. T.S., K.Saku., Y.C. prepared AAV plasmid vectors. T.S. and Y.C.S. prepared the rabies virus vectors. M.A., K.Saki., and T.S. generated *Npbwr1*$^{+/Cre}$ mice. S.S. performed statistical analyses. S.S. and T.S. prepared the manuscript. **Competing interests:** The authors declare that they have no competing interests. **Data and materials availability:** All data needed to evaluate the conclusions in the paper are present in the paper and/or the Supplementary Materials. Plasmids and AAVs with Addgene numbers listed in Materials and Methods were obtained under a material transfer agreement with Addgene. The Npbwr1-iCre mice can be provided by T.S. pending scientific review and a completed material transfer agreement. Requests for the plasmids, AAVs, and Npbwr1-iCre mice should be submitted to mta@addgene.org and sakurai.takeshi.gf@u.tsukuba.ac.jp.

Submitted 24 November 2023
Accepted 12 December 2024
Published 15 January 2025
10.1126/sciadv.adn1335